The Nonlinear Interactions and Maintenance of the Large-Scale Moving Waves in the Atmosphere

S. K. KAO AND H. N. LEE

Department of Meteorology, University of Utah, Salt Lake City 84112

(Manuscript received 24 May 1976, in revised form 22 November 1976)

ABSTRACT

An analysis of the linear and nonlinear interactions of atmospheric motion in the wavenumber-frequency domain indicates that the kinetic energy of the large-scale moving waves is essentially maintained by the nonlinear interactions and the pressure force. In middle latitudes where an eastward mean zonal flow prevails, the supply of kinetic energy to eastward moving waves through the nonlinear interactions is greater than the extraction of kinetic energy through the pressure force, whereas the supply of kinetic energy to westward moving waves through the pressure force is greater than the extraction of kinetic energy through the nonlinear interactions. Near the equator where a weak westward mean zonal flow occurs, the nonlinear interactions generally extract kinetic energy from the eastward moving waves, but supply kinetic energy to the westward moving waves; the pressure force, however, supplies kinetic energy to both eastward and westward moving waves.

The primary contribution of the nonlinear interactions to the energy transfer in wavenumber-frequency domain is essentially through the interactions of the slowly moving waves, the stationary long waves and the zonal mean flow. The interactions between the stationary long waves and waves moving in the same (opposite) direction of the mean zonal flow generally extract (supply) kinetic energy from (to) the moving waves, whereas the interactions between the mean zonal flow and waves moving in the same (opposite) direction of the zonal flow generally supply (extract) kinetic energy to (from) the moving waves.

1. Introduction

Analyses of energy transfers in a fluid are basic in the understanding of the mechanism for the wave motion in the fluid. For unstable waves of small amplitude moving in a stationary parallel flow, it is known that the transfer of kinetic energy is generally from the mean flow to the waves. However, for waves of finite amplitude the transfer of energy due to nonlinear interactions becomes very complex. Analyses of nonlinear interactions of atmospheric waves in the wavenumber domain indicate that practically all waves transfer their kinetic energy to the mean flow, except that waves of wavenumber 3 receive energy from the mean flow (e.g., Steinberg *et al.*, 1971). In view of the fact that atmospheric waves of various wavelengths move at different phase velocities, questions arise as to whether energy transfer between these waves and the mean flow behaves similarly to that in the wavenumber domain and how these waves are maintained. The main purpose of this paper is to make such a study.

To analyze the characteristics of motions and energy transfer in waves of various wavelengths and phase velocities, it is appropriate to examine the behavior of wave motions in the wavenumber-frequency domain. In an earlier paper (Kao, 1968), the governing equations for large-scale atmospheric motion were transformed from physical space to the wavenumber-frequency domain. With the use of these equations a preliminary analysis of the energy spectra, the linear and the nonlinear interactions of atmospheric waves in the wavenumber frequency domain has been made (Wendell, 1969; Kao and Wendell, 1970; Kao *et al.*, 1970). Because of the rather involved computation, the nonlinear interactions were analyzed only at 40°N at 500 mb. The results obtained were insufficient for the analysis of the mechanism for the maintenance of moving waves in the atmosphere. In this paper, we analyze the linear and nonlinear interaction in the tropics, subtropics and middle latitudes.

2. Method and data

There are essentially two methods of computing a wavenumber-frequency spectrum: the direct Fourier transform method (Kao, 1968) which gives a discrete spectrum and the correlation-transform method (Hayashi, 1971) which gives a smoothed spectrum. Tsay (1974a) and Pratt (1976) have shown that the two methods are equivalent at a discrete frequency, and that, in practice, to obtain a smoothed spectrum one may apply a direct frequency smoothing to the Fourier component computed using Kao's method, or use a lag window in a lag correlation analysis using Hayashi's method. The two smoothing techniques are essentially equivalent (Koopmans, 1974). The method of direct Fourier transform with frequency smoothing, which has been used by Tsay (1974b) and Gruber (1975) in their analyses of wave motion in the NCAR general circulation model and in the tropics, is employed in the computation of wavenumber-frequency spectra in this study.

The procedure of the spectrum computation may be summarized as follows: Let $Q(k,\pm n)$ be the complex Fourier coefficient of an atmospheric variable $q(\lambda,t)$ which is a function of longitude λ and time t, where $Q(k,\pm n)=Q_r(k,\pm n)+iQ_i(k,\pm n)$ and k and n stand for wavenumber and frequency; then the real and imaginary parts of $Q(k,\pm n)$ are

$$\left.\begin{aligned} Q_r(k,\pm n)&=\frac{1}{4\pi^2}\int_0^{2\pi}\int_0^{2\pi} q(\lambda,t)\cos(k\lambda\pm nt)d\lambda dt \\ Q_i(k,\pm n)&=-\frac{1}{4\pi^2}\int_0^{2\pi}\int_0^{2\pi} q(\lambda,t)\sin(k\lambda\pm nt)d\lambda dt \end{aligned}\right\}. \quad (1)$$

It is seen in (1) that the positive sign of frequency represents the wave traveling westward and the negative sign eastward. Time t is in normalized form $[t=(2\pi/T)t']$ with the entire observational record period T and real time t'.

It can be shown that the Fourier coefficients may be computed as follows:

1) Take the Fourier transform of $q(\lambda,t)$ in space

$$\left.\begin{aligned} \tfrac{1}{2}C_q(k,t)&=\frac{1}{2\pi}\int_0^{2\pi} q(\lambda,t)\cos(k\lambda)d\lambda \\ \tfrac{1}{2}S_q(k,t)&=-\frac{1}{2\pi}\int_0^{2\pi} q(\lambda,t)\sin(k\lambda)d\lambda \end{aligned}\right\}. \quad (2)$$

2) Compute the Fourier transform of $C_q(k,t)$ and $S_q(k,t)$ in time for each wavenumber and $Q(k,\pm n)$ using the form

$$\left.\begin{aligned} Q_r(k,\pm n)&=\frac{1}{2}\frac{1}{2\pi}\left[\int_0^{2\pi} C_q(k,t)\cos(nt)dt \pm\int_0^{2\pi} S_q(k,t)\sin(nt)dt\right] \\ Q_i(k,\pm n)&=\frac{1}{2}\frac{1}{2\pi}\left[\int_0^{2\pi} S_q(k,t)\cos(nt)dt \mp\int_0^{2\pi} C_q(k,t)\sin(nt)dt\right] \end{aligned}\right\}. \quad (3)$$

Note that both (2) and (3) can be computed by the fast Fourier transform technique.

Then the wavenumber frequency spectrum may be computed as

$$E_{pq}(k,\pm n)=2[P_r(k,\pm n)Q_r(k,\pm n)+P_i(k,\pm n)Q_i(k,\pm n)], \quad (4)$$

where $P(k,\pm n)=P_r(k,\pm n)+iP_i(k,\pm n)$ is the Fourier coefficient for a variable $p(\lambda,t)$. $E_{pq}(k,\pm n)$ is a power spectrum if $p(\lambda,t)\equiv q(\lambda,t)$, while $E_{pq}(k,\pm n)$ is the cross spectrum of p and q if $p(\lambda,t)\not\equiv q(\lambda,t)$.

The procedure of computation involves, first, the calculation of Fourier coefficients $C_q(k,t)$ and $S_q(k,t)$ in (2) by applying the fast Fourier transform, next the computation of the wavenumber-frequency spectrums with the use of (3) by removing the mean and linear trend, and finally the application of the so-called "tapering" spectral window (Tukey, 1967) to the spectra.

The horizontal velocities used in this analysis are derived from the 1973–74 National Meteorological Center (NMC) streamfunction analysis at 200 and 500 mb. The streamfunction is constructed with the use of conventional, as well as aircraft and satellite, data. The wind velocities are calculated from the streamfunction differences taken over 5° of latitude or longitude, centered about the desired location of the wind. The 5° latitude-longitude square is the basic grid employed in this analysis technique and is completely described in a discussion on the analysis scheme devised for computations within this area in a paper by Bedient *et al.* (1967). The time interval used in the integration is 12 h over a period of 90 days for the winter season 1 December 1973 to 1 March 1974.

3. Latitudinal distribution of mean zonal velocity, meridional flux of westerly momentum and kinetic energy of the stationary and transient waves

The wavenumber-frequency spectra of the zonal and meridional components of velocities at 200 mb (winter 1973) have been computed for each 5° latitude circle in the latitude belt between 33°S and 80°N. In view of the importance of the relationship between the mean zonal motion and the kinetic energy of wave motions in the atmosphere, the latitudinal distribution of the zonal mean velocity, the meridional flux of westerly momentum and the kinetic energy of stationary and transient waves, at 200 mb for the winter season of 1973, are shown in Figs. 1a–1d. Fig. 1a indicates that at 200 mb a light easterly mean zonal wind occurred between the equator and 15.5°S, and that outside this latitudinal belt westerly zonal mean flow prevailed with a maximum wind speed of 37.7 m s^{-1} located at about 33°N, which agrees well with earlier observations (Lorenz, 1967). Figs. 1b and 1c show the latitudinal distribution of the kinetic energy of the stationary and moving waves (for wavenumbers 1–15) of the zonal and meridional motion, respectively. It may be noted

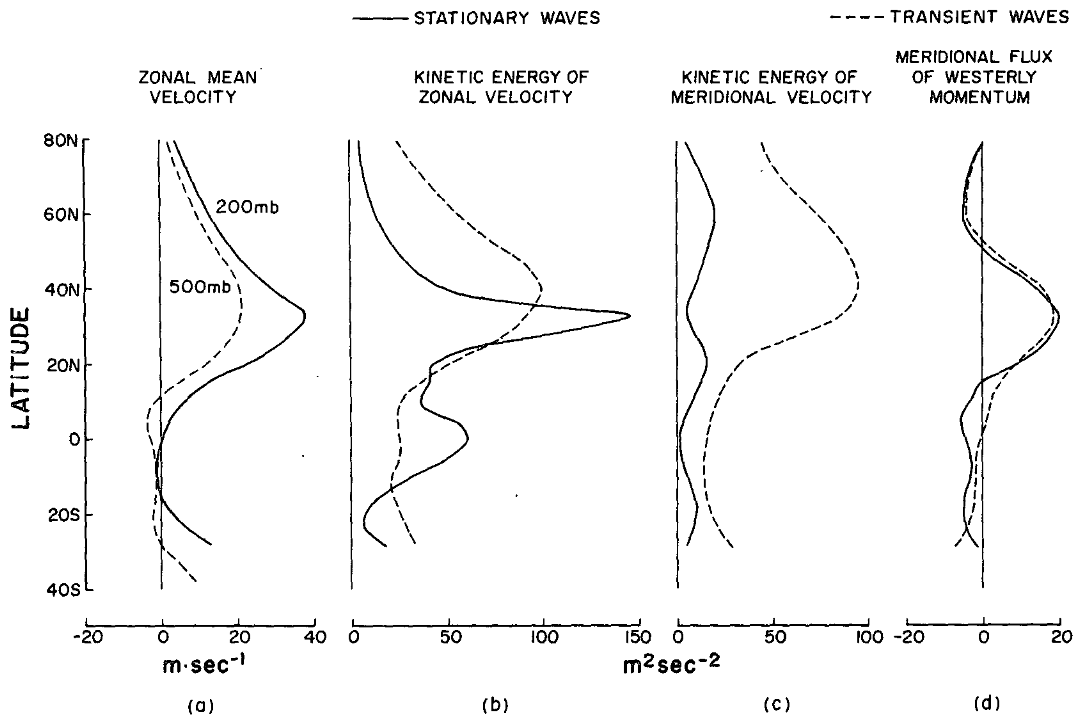

FIG. 1. Latitudinal distribution of mean zonal velocity (a), kinetic energy of the zonal (b) and meridional (c) velocities associated with the stationary and moving waves, and meridional flux of westerly momentum (d) at 200 mb, winter 1973.

that 1) the kinetic energy of the stationary waves of the zonal motion is greater than that of the meridional motion, 2) the former shows two maxima, a major maximum near 33°N and a secondary one near the equator, 3) the latitudinal distribution of the kinetic energy of the moving waves of the zonal motion is very similar to that of the meridional motion, indicating that the kinetic energy of the moving waves distributes almost equally in the zonal and meridional motions, and 4) a maximum of the kinetic energy of the moving waves occurs near 40°N, approximately 7° north of the maximum of the zonal mean motion.

Fig. 1d shows that 1) north of 20°N the latitudinal distribution of the meridional flux of the westerly

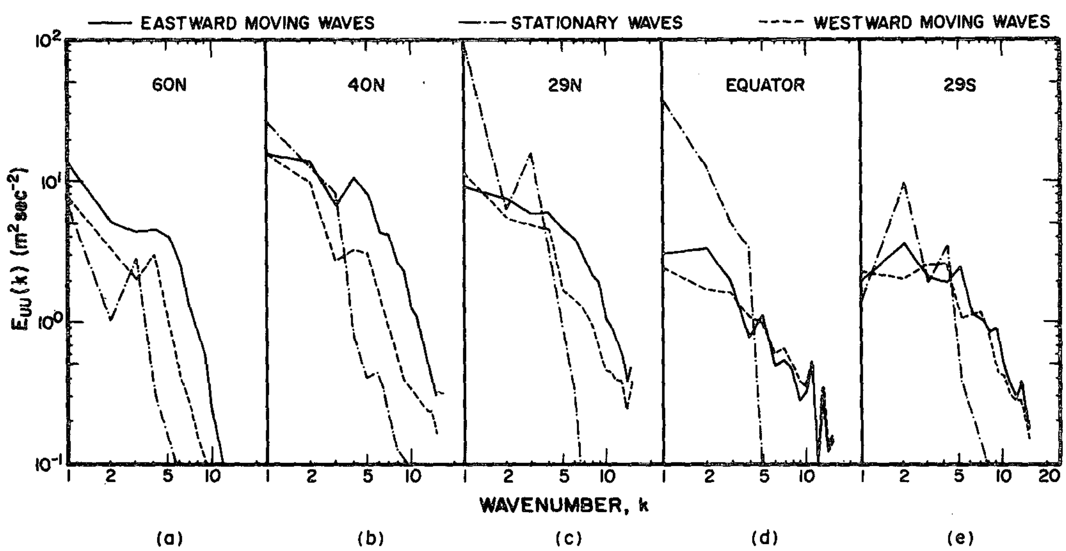

FIG. 2. Latitudinal variation of wavenumber spectra of the zonal motion associated with stationary and moving waves at 200 mb, winter 1973.

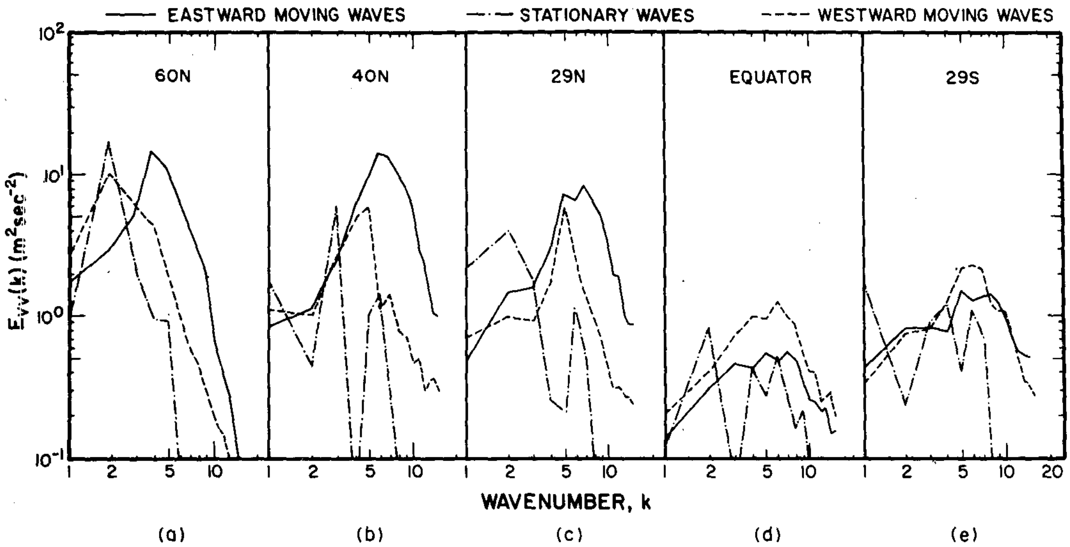

FIG. 3. As in Fig. 2 except for the meridional motion.

momentum associated with the stationary waves is very similar to that with the moving waves, with a maximum northward flux of westerly momentum occurring near 33°N (near the maximum of the zonal mean flow) and a maximum southward momentum flux occurring near 60°N, and 2) between 15°N and 30°S, the meridional flux of the westerly momentum is generally toward the south.

4. Energy spectra of the zonal and meridional motions

To analyze the motion of atmospheric waves in the wavenumber-frequency domain, we shall first examine the wave characteristics in the wavenumber domain. The wavenumber spectra of the zonal and meridional velocities for the stationary, westward and eastward moving waves at 29°S, the equator, 29°N, 40°N and 60°N are computed and shown in Figs. 2 and 3. Fig. 2 indicates that: 1) the spectral energy of the zonal motion generally decreases with increasing wavenumber, and is approximately proportional to k^{-3} to k^{-4} in the large wavenumber range [Kraichnan (1967), Leith (1968, 1971), Lilly (1969), Kao (1970) and Charney (1971) have shown that for two-dimensional isotropic turbulence the energy spectrum varies as k^{-3} in the enstrophy transfer range]; 2) near the equator the spectral energy of the zonal motion of stationary waves is generally greater than that of the moving waves in the small wavenumber range; 3) outside the tropics, in the high wavenumber range, the spectral energy of

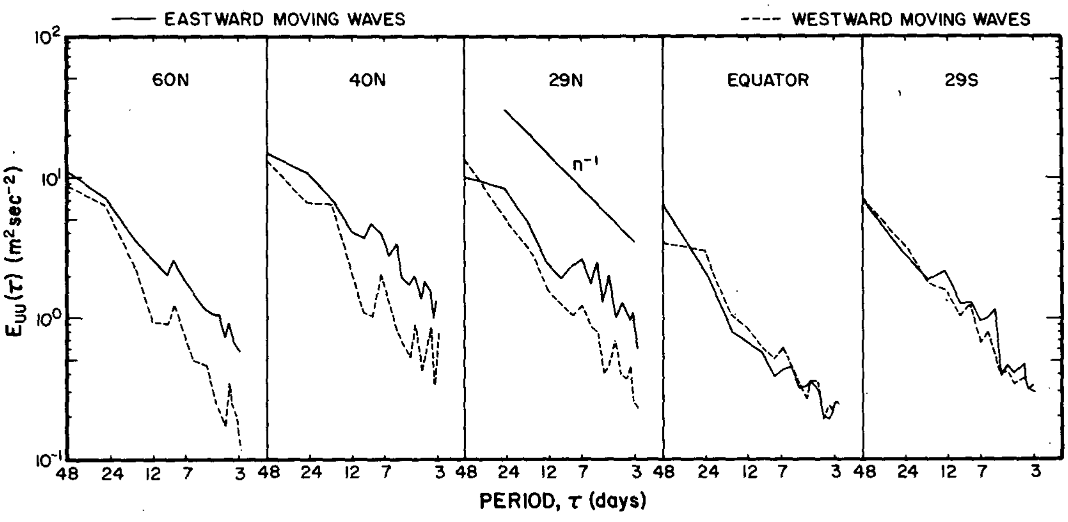

FIG. 4. Latitudinal variation of frequency spectra of the zonal motion at 200 mb, winter 1973.

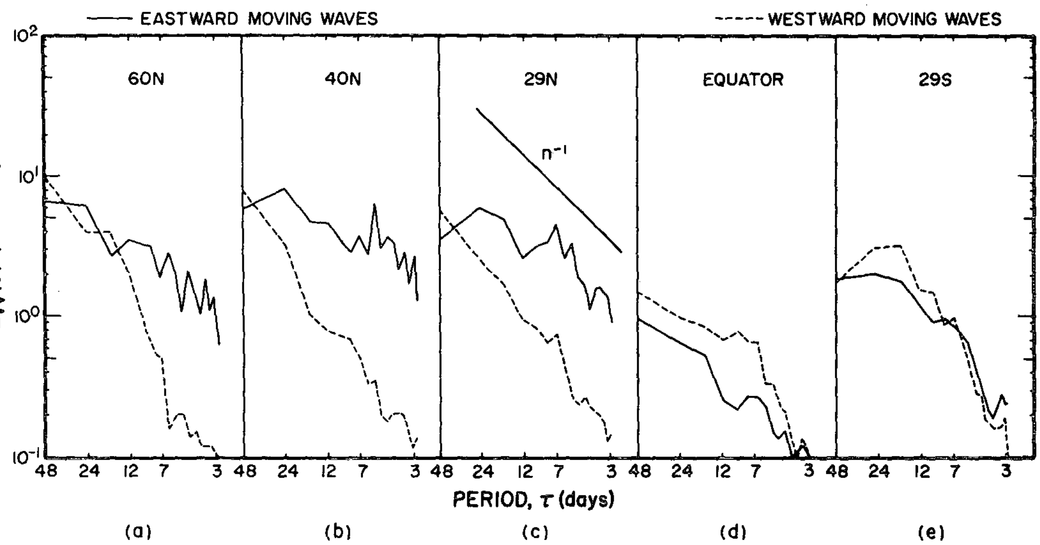

FIG. 5. As in Fig. 4 except for the meridional motion.

the zonal motion of the eastward moving waves is greater than that of the westward-moving waves, and the latter is greater than the spectral energy of the stationary waves.

Fig. 3 shows that 1) near the equator more kinetic energy of the meridional motion is associated with the westward-moving waves than with the eastward-moving and stationary waves, and 2) in the middle and high latitudes more spectral energy of the meridional motion is associated with the eastward-moving waves in the medium wavenumber range (5–10) and associated with the stationary waves in the small wavenumber range.

To complement the analysis of the wavenumber spectra of atmospheric waves, the frequency spectra of the zonal and meridional motion for the eastward and westward moving waves at 200 mb (winter 1973) are computed and shown in Figs. 4 and 5. These two figures indicate that energy spectra in the frequency domain are approximately proportional to the −1 power of the frequency. In regions near the equator

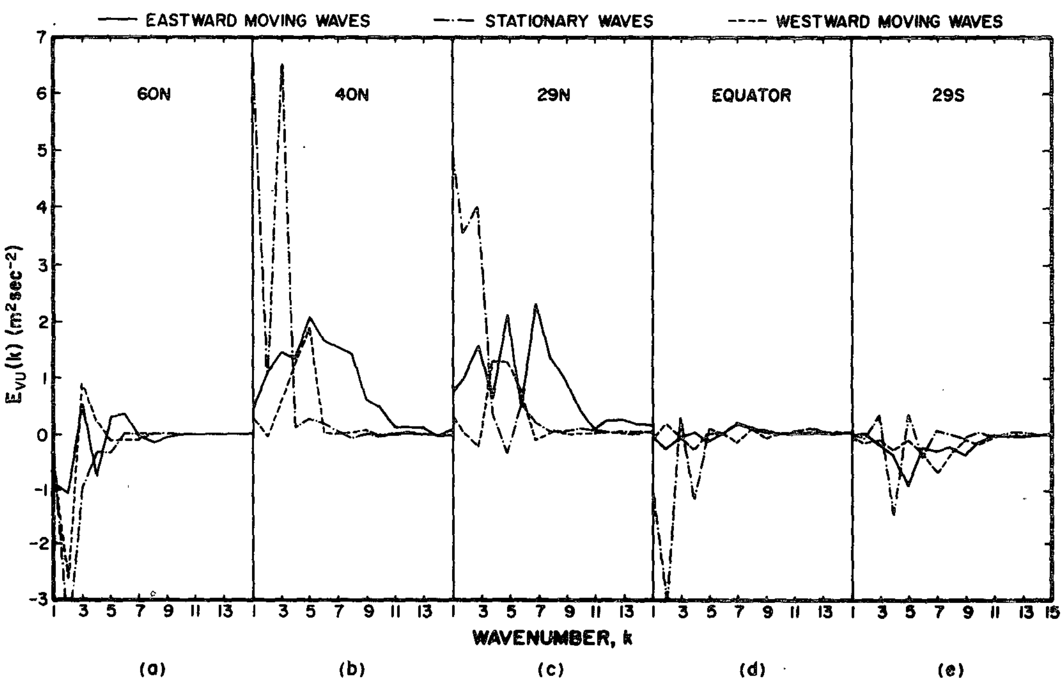

FIG. 6. Latitudinal variation of wavenumber cospectra of the meridional flux of westerly momentum per unit mass, associated with stationary and moving waves at 200 mb, winter 1973.

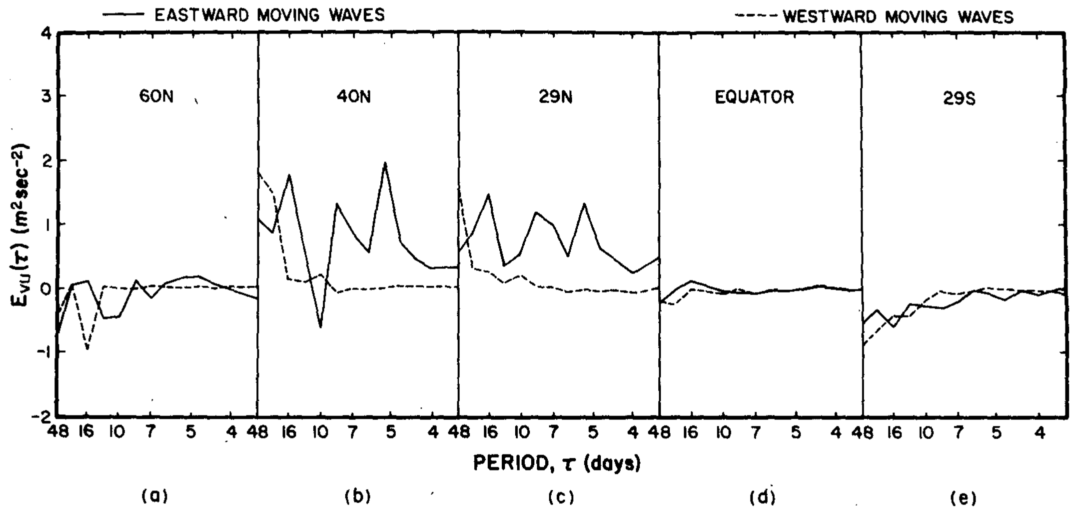

FIG. 7. As in Fig. 6 except for frequency cospectra.

the spectral energy of both the zonal and meridional motions associated with westward moving waves is generally greater than that with eastward moving waves; however, the reverse is true outside the latitudinal belt between 20°N and 29°S.

5. Characteristics of cospectra of the meridional flux of westerly momentum

The wavenumber cospectra of the meridional flux of westerly momentum at 60°N, 40°N, 29°N, the equator and 29°S (at 200 mb, winter 1973) are shown in Fig. 6. This figure indicates that the momentum flux is mostly accomplished by long atmospheric waves. It may be noted that in high latitudes the meridional flux of westerly momentum is essentially associated with stationary waves of wavenumber 2 and in middle latitudes with stationary waves of wavenumbers 1, 2, 3 and with transient waves in the wavenumber range 2 to 9. At the equator, the momentum flux is essentially associated with stationary waves of wavenumbers 2 and 4. At 29°S it is primarily associated with stationary waves of wavenumbers 4 and 7 and with transient waves of wavenumber 5.

The frequency cospectra of the meridional flux of westerly momentum at 60°N, 40°N, 29°N, the equator and 29°S (at 200 mb, winter 1973), are shown in Fig. 7. These spectra show that transient waves contributed little to the momentum transport near the equator, and that in middle latitudes most of the momentum flux is associated with the eastward moving waves of period 5, 8 and 16 days and with the westward moving waves of low frequency. At 60°N and 29°S, however, it is essentially associated with moving waves of low frequencies.

6. Equations for kinetic energy and meridional flux of westerly momentum in wavenumber-frequency space

To analyze the effect of the nonlinear interactions on the kinetic energy and meridional flux of westerly momentum, we consider the kinetic energy equations for the zonal and meridional components of the motion, and the equation for the meridional flux of westerly momentum:

$$\frac{1}{2}\frac{\partial u^2}{\partial t}=\underset{(u1)}{-\frac{u^2}{a\cos\phi}\frac{\partial u}{\partial\lambda}}\underset{(u2)}{-\frac{uv}{a}\frac{\partial u}{\partial\phi}}\underset{(u3)}{+\frac{\tan\phi}{a}u^2v}\underset{(u4)}{+fu(v-v_g)}\underset{(u5)}{+uF_1},\qquad(5)$$

$$\frac{1}{2}\frac{\partial v^2}{\partial t}=\underset{(v1)}{-\frac{uv}{a\cos\phi}\frac{\partial v}{\partial\lambda}}\underset{(v2)}{-\frac{v^2}{a}\frac{\partial v}{\partial\phi}}\underset{(v3)}{-\frac{\tan\phi}{a}u^2v}\underset{(v4)}{-fv(u-u_g)}\underset{(v5)}{+uF_2},\qquad(6)$$

$$\frac{\partial}{\partial t}(vua\cos\phi)=-\frac{\partial}{\partial\lambda}(u^2v)-\frac{\partial}{\partial\phi}(uv^2\cos\phi)-a\cos\phi\frac{\partial}{\partial p}(uv\omega)-a\cos\phi f(u^2-v^2)-g\sin\phi(u^2-v^2)u-g\cos\phi\left(\frac{v}{\cos\phi}\frac{\partial z}{\partial\lambda}+u\frac{\partial z}{\partial\phi}\right)+a\cos\phi(vF_1+uF_2),\qquad(7)$$

where z is the geopotential height of the isobaric surface,

u and v are the zonal and meridional components, respectively, of the velocity, u_g and v_g the zonal and meridional components, respectively, of the geostrophic velocity and F_1 and F_2 the x and y components of the sum of the molecular and eddy stress forces (Kao, 1968).

To obtain the equations corresponding to (5), (6) and (7) in wavenumber-frequency space, we introduce the following notation for the Fourier coefficients:

$$\frac{q(\lambda,t,p,\phi)}{Q(k,n,p,\phi)}\left|\frac{u\quad v\quad \omega\quad z\quad F_1\quad F_2}{U\quad V\quad W\quad Z\quad G_1\quad G_2}\right..$$

It can be shown that the equations for kinetic energy and meridional flux of westerly momentum in wavenumber-frequency space take the form (Kao, 1968)

$$\underset{(EUU)}{|U(k,n)|^2}=\frac{T}{2\pi}\left\{\underset{(U1)}{U(-k,\,-n)\frac{i}{n}\sum_j\sum_m\left[\frac{i}{a\cos\phi}jU(j,m)U(k-j,\,n-m)\right]}\right.$$
$$+\underset{(U2)}{U(-k,\,-n)\frac{i}{na}\sum_j\sum_m[U_\phi(j,m)V(k-j,\,n-m)]}$$
$$-\underset{(U3)}{U(-k,\,-n)i\frac{\tan\phi}{na}\sum_j\sum_m[U(j,m)V(k-j,\,n-m)]}$$
$$\left.-\underset{(U4)}{U(-k,\,-n)\frac{i}{n}f[V(k,n)-V_g(k,n)]}-\underset{(U5)}{\frac{i}{n}U(-k,\,-n)G_1(k,n)}\right\},\quad (8)$$

$$\underset{(EVV)}{|V(k,n)|^2}=\frac{T}{2\pi}\left\{\underset{(V1)}{V(-k,\,-n)\frac{i}{n}\sum_j\sum_m\frac{i}{a\cos\phi}[jV(j,m)U(k-j,\,n-m)]}\right.$$
$$+\underset{(V2)}{V(-k,\,-n)\frac{i}{na}\sum_j\sum_m[V_\phi(j,m)V(k-j,\,n-m)]}$$
$$+\underset{(V3)}{V(-k,\,-n)\frac{i\tan\phi}{na}\sum_j\sum_m[U(j,m)U(k-j,\,n-m)]}$$
$$\left.+\underset{(V4)}{V(-k,\,-n)\frac{i}{n}f[U(k,n)-U_g(k,n)}-\underset{(V5)}{\frac{i}{n}V(-k,\,-n)G_2(k,n)}\right\},\quad (9)$$

$$\underset{(EVU)}{\frac{2\pi a^2\cos^2\phi}{g}E_{uv}(k,n)}=\frac{aT\cos^2\phi}{gn}\left\{\underset{(VU1)}{\frac{-1}{\cos\phi}\sum_j\sum_m jU(k-j,\,n-m)[U(j,m)V(-k,\,-n)+V(j,m)U(-k,\,-n)]}\right.$$
$$+\underset{(VU2)}{i\sum_j\sum_m V(k-j,\,n-m)[U_\phi(j,m)V(-k,\,-n)+V_\phi(j,m)U(-k,\,-n)]}$$
$$\left.+\underset{(VU3)}{i\tan\phi\sum_j\sum_m U(j,m)[U(-k,\,-n)U(k-j,\,n-m)-V(-k,\,-n)V(k-j,\,n-m)]}\right\}$$
$$+\underset{(VU4)}{\frac{ifTa^2\cos^2\phi}{gn}\{U(-k,\,-n)[U(k,n)-U_g(k,n)]-V(-k,\,-n)[V(k,n)-V_g(k,n)]\}}$$
$$+\underset{(VU5)}{\frac{iTa^2\cos^2\phi}{gn}\{U(-k,\,-n)G_2(k,n)-V(-k,\,-n)G_1(k,n)\}}$$
$$+\frac{iTa\cos^2\phi}{gn}\{\sum_j\sum_m W(k-j,\,n-m)[U_p(j,m)U(-k,\,-n)+V_p(j,m)V(-k,\,-n)]\}.\quad (10)$$

TABLE 1. Wavenumber partition.

Wavenumber k	Classification	Symbol
0	zonally averaged flow	0
1–5	long waves (small wavenumber)	k_s
6–9	medium waves	k_m
10–20	short waves (large wavenumber)	k_L

where U_g and V_g are the transforms of the zonal and meridional components of the geostrophic velocity. The symbols below the terms on the right-hand side of the above equation are for future reference. The summations over the index j are from $-j_s$ to $+j_s$, where j_s depends on the number of discrete points on the latitude circle. The summations over m are from $\mp m_s$ to $\pm m_s$ depending on whether frequency n is positive or negative, where m_s depends on the number of discrete time points used. Summation is used here in place of integration with respect to m because the transforms are computed for integer values of frequency.

Eq. (8) shows that the kinetic energy associated with the zonal velocity of the moving waves of wavenumber k and frequency n is maintained by the nonlinear interactions, with $U1$ and $U2$ corresponding, respectively, to the longitudinal and latitudinal convergence of energy flux, $U3$ to the sphericity effect, and $(U4+U5)$ to the effect of velocity deviation from the geostrophic (the Reynolds-stress force including cumulative computational errors) which can be determined by the balance of all the other terms in (8). Similarly, (9) shows that the kinetic energy associated with the meridional velocity of the moving waves of wavenumber k and frequency n is maintained by $V1$, $V2$, $V3$ and $(V4+V5)$, whereas (10) shows that the spectral meridional flux of zonal angular momentum is maintained by $VU1$, $VU2$, $VU3$ and $(VU4+VU5)$. The reason that we do not compute $U4$, $V4$ and $VU4$ separately is due to the fact that computations of these terms need pressure-height data which are not available in the tropics.

7. Wavenumber and frequency partitions

The transformation of the nonlinear terms of the kinetic energy and momentum flux equations into wavenumber-frequency space results in terms which involve sums of products of transforms for various waves and frequencies. For example, the transformed longitudinal convergence of momentum flux involves

$$\sum_{j=-j_s}^{j_s} \sum_{m=-m_s}^{m_s} jU(j,m)U(k-j,\, n-m), \qquad (11)$$

where for computations over 90-day seasons the upper and lower limits of wavenumber and frequency used are $j_s=\pm 20$ and $m_s=\pm 90$, respectively. It may be noted from (11) that depending on the values of k and n the term will involve from 1800 to 7200 products of transforms. Each product may be considered an interaction between the wavenumbers and frequencies represented by (j,m) and $(k-j,\, n-m)$. Because of the extremely large number of possible interactions, it is necessary for analysis purposes to make use of a system of classification which divides the wavenumber-frequency space into particular domains as shown in Tables 1 and 2.

From the classifications in Tables 1 and 2, according to wavenumber and frequency, it may be noted that there are 28 domains which may interact with each other and themselves for a total of 406 possible interaction combinations. Each domain is designated by combining the symbols used for the wavenumber and frequency classifications. For example, the domain of long waves moving from west to east with medium frequency would be represented by $(k_s, +n_m)$. The interaction combinations are designated by placing the scale-frequency category symbols side by side, e.g., $(k_s, +n_m)(k_m, -n_L)$.

8. Nonlinear interactions and maintenance of spectral energy in moving waves

The values of the terms in the spectral energy equations (8) and (9) have been computed for each wavenumber-frequency domain at the equator, 20°N and 40°N, representing the tropics, the subtropics and midlatitudes. For the calculation of the linear and nonlinear interaction terms a total of 406 interactions has been computed. To list the linear and nonlinear interactions for various wavenumber-frequency domains at the above-mentioned three latitudes would require more than a hundred tables. To gain an insight into the mechanism for the linear and nonlinear interaction contributions to the spectral kinetic energy in wavenumber-frequency domains, only the spectral energy which is sizable is considered, and the resultant values of the interaction contributions due to the longitudinal and latitudinal convergence of the flux of kinetic energy ($U1$, $V1$, $U2$, $V2$), the earth's sphericity ($U3$, $V3$), and the combined ageostrophic and Reynolds stress forces and cumulative error ($U4+U5$, $V4+V5$)

TABLE 2. Frequency partition.

Frequency n (cycles per 90 days)	Period (days)	Classification (frequency)	Direction of wave motion	Symbol
−90 to −31	1–3	high	west to east	$+n_h$
−30 to −11	3–9	medium	west to east	$+n_m$
−10 to −1	9–90	low	west to east	$+n_L$
0		zero	stationary	0
1 to 10	9–90	low	east to west	$-n_L$
11 to 30	3–9	medium	east to west	$-n_m$
31 to 90	1–3	high	east to west	$-n_h$

TABLE 3. Linear and nonlinear contributions to the energy spectra in various wavenumber-frequency domains at 20°S, the equator, 20°N and 40°N at 500 mb.

		EUU = U1 + U2 + U3 + (U4 + U5)	EVV = V1 + V2 + V3 + (V4 + V5)
$(k_s, +n_L)$	40°N	16.83 = 75.81 − 13.06 − 0.13 − 45.79	7.31 = 48.67 − 15.28 + 4.33 − 30.41
	20°N	8.25 = 22.55 − 8.63 + 0.48 − 6.15	1.81 = 8.64 + 0.58 + 1.19 − 8.61
	0	1.36 = −0.52 + 0.06 + 0.00 + 1.83	0.12 = −0.10 + 0.04 + 0.00 + 0.16
	20°S	3.74 = 1.33 − 1.07 + 0.03 + 3.45	0.54 = 0.22 − 0.00 − 0.02 + 0.34
$(k_s, -n_L)$	40°N	13.39 = −59.85 + 15.79 + 1.09 + 56.36	7.85 = −49.92 + 11.61 + 1.11 + 45.05
	20°N	4.73 = −13.61 + 2.18 − 0.17 + 16.33	1.61 = −6.81 − 0.65 − 0.57 + 10.07
	0	2.62 = 1.67 − 0.25 + 0.00 + 1.20	0.45 = 0.25 − 0.05 + 0.00 + 0.26
	20°S	2.45 = −1.22 + 0.80 + 0.02 + 2.85	0.96 = −0.01 + 0.17 + 0.05 + 0.75
$(k_s, +n_m)$	40°N	7.12 = 8.39 + 1.55 + 0.08 − 4.40	2.56 = 5.31 + 0.29 + 0.31 − 3.35
	20°N	1.11 = 0.45 − 0.14 + 0.01 + 0.78	0.51 = 0.35 + 0.02 + 0.03 + 0.10
	0	0.36 = −0.03 + 0.02 + 0.00 + 0.37	0.11 = −0.02 + 0.00 + 0.00 + 0.12
	20°S	0.59 = 0.00 − 0.03 + 0.00 + 0.61	0.21 = 0.03 + 0.01 − 0.00 + 0.16
$(k_m, +n_L)$	40°N	2.64 = 18.37 − 10.26 − 1.03 − 4.44	5.80 = 32.19 − 0.28 − 2.47 − 23.64
	20°N	1.95 = 13.52 − 3.99 + 0.48 − 8.06	2.32 = 11.86 + 0.04 + 1.12 − 10.70
	0	0.18 = −0.05 − 0.02 + 0.00 + 0.25	0.12 = −0.22 + 0.03 + 0.00 + 0.31
	20°S	1.24 = 1.28 − 1.64 + 0.02 + 1.59	1.18 = 0.79 + 0.07 − 0.06 + 0.38
$(k_m, -n_L)$	40°N	1.12 = −11.15 + 7.60 + 0.28 + 4.29	1.52 = −13.21 + 2.48 + 0.07 + 12.18
	20°N	0.45 = −2.64 − 0.15 − 0.07 + 3.32	0.84 = −5.67 + 0.02 + 0.00 + 6.49
	0	0.55 = 0.16 + 0.07 + 0.00 + 0.32	0.25 = 0.17 − 0.04 + 0.00 + 0.11
	20°N	0.94 = −0.91 + 0.78 + 0.02 + 1.04	1.00 = −0.94 + 0.07 + 0.03 + 1.84
$(k_m, +n_m)$	40°N	3.35 = 6.74 − 1.04 − 0.08 − 2.27	15.11 = 30.40 − 1.63 − 0.29 − 13.37
	20°N	1.53 = 1.61 − 0.69 + 0.05 + 0.55	1.61 = 1.82 + 0.09 + 0.11 − 0.41
	0	0.10 = −0.02 − 0.00 + 0.00 + 0.12	0.08 = −0.02 + 0.00 + 0.00 + 0.10
	20°S	0.37 = 0.26 − 0.07 − 0.01 + 0.19	0.32 = 0.18 + 0.01 − 0.01 + 0.13

are listed in Table 3. In Tables 4, 5 and 6, the primary and secondary nonlinear interaction contributions to the longitudinal and latitudinal convergence of the flux of kinetic energy at the equator, 20°N and 40°N are summarized.

In Table 3, the following characteristics of the linear and nonlinear contributions to the spectral energy in various wavenumber-frequency domains may be noted:

1) The order of magnitude of the nonlinear interaction terms is the same as that of the terms involving the pressure, Coriolis and Reynolds stress forces.

2) In the mid-latitudes and the subtropics, the resultant of nonlinear interactions corresponding to the longitudinal convergence of the flux of kinetic energy ($U1,V1$) supplies kinetic energy to eastward moving waves but extracts kinetic energy from westward moving waves. However, at the equator the reverse is true.

3) The resultant of the nonlinear interactions corresponding to the latitudinal convergence of the flux of kinetic energy ($U2,V2$) is generally smaller than and of the opposite sign to that due to the longitudinal convergence of the flux of kinetic energy ($U1,V1$).

4) In the mid-latitudes and the subtropics, the pressure, Coriolis and Reynolds stress forces (including cumulative computational errors), i.e., ($U4+U5$, $V4+V5$), supply kinetic energy to westward moving waves but extract kinetic energy from eastward moving waves.

5) At the equator where the Coriolis force vanishes, the pressure and Reynolds stress forces (including computational errors), i.e., ($U4+U5$, $V4+V5$), supply

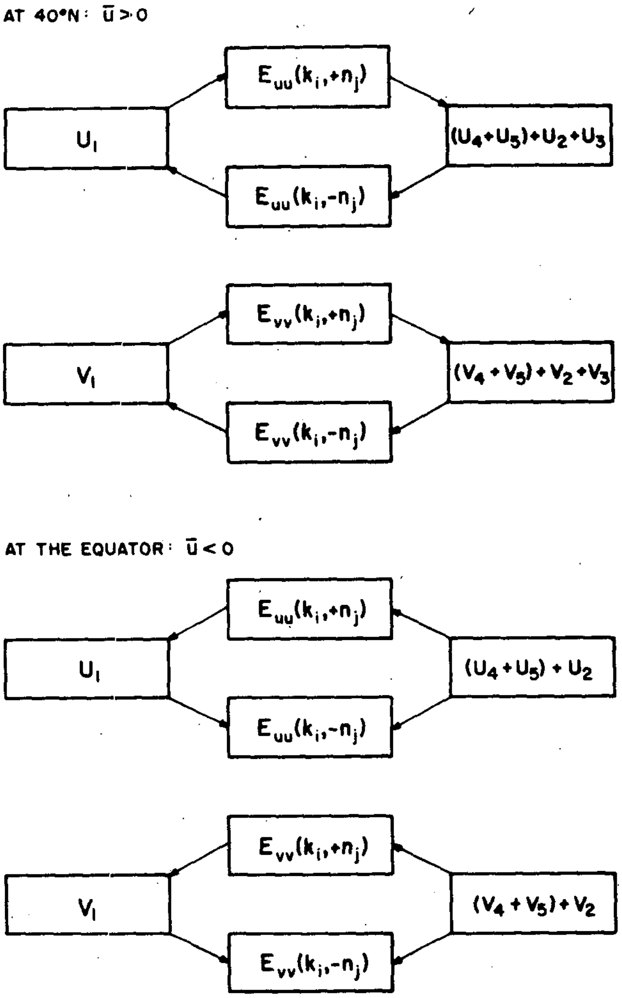

FIG. 8. Schematic diagram for the maintenance of spectral energy of moving waves at 500 mb, winter 1973.

kinetic energy to both eastward and westward moving waves.

6) The sphericity effect of the earth ($U3$, $V3$) is generally small.

Fig. 8 schematically shows the maintenance of the spectral energy of the moving waves as the resultant of the nonlinear interactions and the pressure, Coriolis and Reynolds stress forces. At 40°N in the westerlies, the nonlinear interactions [($U1,V1$) corresponding to the longitudinal convergence of momentum] supply (extract) spectral energy to (from) eastward (westward) moving waves; whereas the pressure, Coriolis and Reynolds stress forces (including computational errors) [($U4+U5$, $V4+V5$)] and the nonlinear interactions [($U2,V2$) corresponding to the meridional convergence of energy flux and ($U3,V3$) due to the effect of sphericity] extract (supply) spectral energy from (to) the eastward (westward) moving waves. At the equator, in the easterlies, however, the nonlinear interactions [($U1,V1$) corresponding to the longitudinal

TABLE 4. Summary of positive and negative nonlinear contributions to $U1$, $U2$, $V1$ and $V2$ in various wavenumber-frequency domains at the equator at 500 mb.

Positive Contributions		Negative Contributions
$(0,0)\ (k_s,-n_L)$ $(0,0)\ (k_m,-n_L)$ $(0,0)\ (k_L,-n_L)$	→ U1 →	$(0,0)\ (k_s,n_L)$ $(0,0)\ (k_L,n_L)$ $(k_s,0)\ (k_s,-n_L)$ $(k_s,0)\ (k_m,-n_L)$
$(0,0)\ (k_s,\pm n_L)$ $(0,0)\ (k_m,-n_L)$ $(k_s,0)\ (k_s,n_L)$ $(k_s,0)\ (0,-n_L)$	→ U2 →	$(0,0)\ (k_m,n_L)$ $(k_s,0)\ (0,n_L)$ $(k_s,0)\ (k_L,n_L)$
$(0,0)\ (k_m,-n_L)$ $(0,0)\ (k_s,-n_L)$ $(0,0)\ (k_L,-n_L)$	→ V1 →	$(0,0)\ (k_s,n_L)$ $(0,0)\ (k_m,n_L)$ $(0,0)\ (k_L,n_L)$ $(k_s,0)(k_m,-n_L)$
(small)	→ V2 →	(small)

convergence of the energy flux] extract (supply) spectral energy from (to) eastward (westward) moving waves, whereas the pressure and Reynolds stress forces (including computational errors), i.e., ($U4+U5$) and ($V4+V5$), and the nonlinear interactions [($U2,V2$), corresponding to the meridional convergence of momentum] supply spectral energy to both the eastward and westward moving waves.

In Tables 4–6 the primary (underlined) and secondary interactions are, respectively, classified according to the interaction values being greater than 2.0 and between 0.5 and 2.0 $m^2\ s^{-2}$ for interactions at the equator and 20°N, and according to interaction values greater than 10.0 and between 3.0 and 10.0 $m^2\ s^{-2}$ for interactions at 40°N.

It may be noted that at the equator and 20°N nonlinear interactions due to the longitudinal and latitudinal convergence of the flux of kinetic energy involve primarily interactions of low-frequency waves of various wavelengths with the zonal mean flow and with stationary long waves. At 40°N, however, the nonlinear interactions involve primarily the zonal mean flow interacting with low-frequency waves of long and medium wavelengths, and interactions between eastward and westward moving long waves of low frequencies.

It is also found that at the equator and 20°N interactions between zonal mean flow and westward (eastward) moving low-frequency waves generally supply (extract) kinetic energy to (from) the westward (eastward) moving low-frequency waves, whereas inter-

TABLE 5. As in Table 4 except at 20°N.

Positive Contributions		Negative Contributions	Positive Contributions		Negative Contributions
$(0,0)\ (k_s,-n_L)$		$(k_s,0)\ (k_s,-n_L)$	$(0,0)(k_L,-n_L)$		$(k_s,0)(k_s,-n_L)$
$(k_s,0)\ (k_s,+n_L)$		$(0,0)\ (k_s,+n_L)$	$(k_s,0)(k_L,n_L)$		$(k_s,0)(k_m,-nL)$
$(k_s,0)\ (0,-n_L)$		$(0,0)\ (k_m,n_L)$	$(0,0)(k_s,-n_L)$		$(k_s,0)(k_L,-n_L)$
$(0,0)\ (k_m,-n_L)$	→ U1 →	$(0,0)\ (k_L,n_L)$	$(0,0)(k_m,-n_L)$	→ V1 →	$(0,0)(k_L,n_L)$
$(0,0)\ (k_L,-n_L)$		$(k_s,0)(k_s,n_L)$	$(k_s,0)(k_s,-n_L)$		$(k_s,0)(k_L,-n_L)$
$(k_s,0)(k_L,-n_L)$		$(k_s\pm n_L)(0,\mp n_L)$	$(k_s,0)(k_m,-n_L)$		$(k_s,0)(k_L,-n_L)$
$(k_s,0)(k_m,+n_L)$		$(k_s,-n_L)(0,-n_L)$	$(k_s,n_L)(k_m,n_L)$		$(k_s,\pm n_L)(k_L,-n_L)$
$(k_s,0)\ (0,n_L)$			$(k_s,n_L)(k_L,\pm n_L)$		$(k_s,n_L)(k_L,n_L)$
$(k_s,+n_L)(k_s,\pm n_L)$			$(k_m,-n_L)(k_L,-n_L)$		
$(k_s,-n_L)(0,n_L)$			$(k_L,-n_L)(k_L,-n_L)$		
			$(k_L,n_L)(0,n_L)$		

Positive Contributions		Negative Contributions	Positive Contributions		Negative Contributions
$(0,0)(k_s,-n_L)$		$(k_s,0)(0,-n_L)$	$(k_s,0)(k_s,-n_L)$	→ V2 →	(small)
$(k_s,0)(0,n_L)$		$(0,0)(k_s,n_L)$			
$(0,0)(k_s,-n_L)$		$(k_s,0)(k_m,n_L)$			
$(0,0)(k_m,-n_L)$	→ U2 →	$(k_s,+n_L)(k_s,+n_L)$			
$(0,0)(k_L,-n_L)$		$(k_s,+n_L)(k_m,0)$			
$(k_s,0)(k_s,n_L)$		$(k_s,-n_L)(k_s,-n_L)$			
$(k_s,0)(k_s,\pm n_L)$					
$(k_s,-n_L)(k_m,-n_L)$					

actions between the stationary long waves and the westward (eastward) moving low-frequency waves generally extract (supply) kinetic energy from (to) the westward (eastward) moving low-frequency waves. At 40°N, the above-mentioned primary interactions still hold except that the process of supply and extraction of kinetic energy reverses. Based on these results an interaction model for primary nonlinear interactions is shown in Fig. 9.

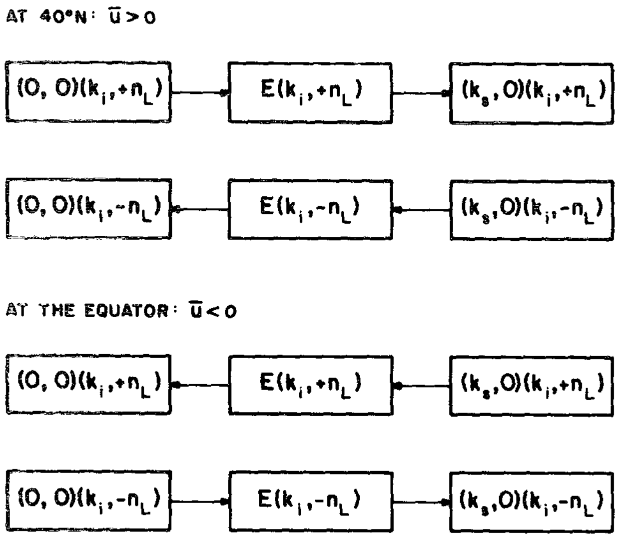

FIG. 9. Schematic diagram for the primary contributions of nonlinear interactions to the spectral energy of moving waves at 500 mb, winter 1973.

9. Nonlinear interactions and maintenance of the spectral meridional flux of westerly momentum in moving waves

The values of the terms of the spectral equation (10) have been computed in each wavenumber-frequency domain at 20°S, the equator, 20°N and 40°N. The interaction terms have each been computed for 406 interaction contributions. Table 7 summarizes the resultant values of the interaction contributions corresponding to the longitudinal and latitudinal convergence of the meridional flux of westerly momentum (*VU*1,*VU*2), the earth's sphericity (*VU*3), and the pressure, Coriolis, Reynolds stress forces and cumulative errors (*VU*4+*VU*5) at 20°S, the equator, 20°N and 40°N. In this table the following characteristics of the linear and nonlinear contributions to meridional flux of westerly momentum in various wavenumber frequency domains may be noted:

1) Except for the eastward slowly moving waves of medium wavelengths at 40°N, the spectral meridional

TABLE 6. As in Table 4 except at 40°N.

Positive Contributions		Negative Contributions
$(0,0)(k_s,n_L)$ $(0,0)(k_m,n_L)$ $(k_s,0)(k_s,-n_L)$ $(k_s,0)(k_s,n_m)$ $(k_s,n_L)(k_s,-n_L)$ $(0,0)(k_m,n_m)$	U1	$(0,0)(k_s,-n_L)$ $(0,0)(k_m,-n_L)$ $(k_s,0)(k_s,n_L)$
$(k_s,n_L)(k_s,-n_L)$ $(0,0)(k_s,n_L)$ $(k_s,0)(k_s,-n_L)$ $(k_m,0)(k_m,\pm n_L)$ $(k_m,n_L)(k_m,-n_L)$	U2	$(k_s,0)(k_s,\pm n_L)$ $(k_s,0)(0,-n_L)$ $(k_s,n_L)(k_s,\pm n_L)$ $(k_s,0)(k_m,n_L)$ $(k_m,n_m)(k_m,-n_m)$
$(0,0)(k_s,n_L)$ $(0,0)(k_m,n_L)$ $(0,0)(k_s,n_m)$ $(k_s,0)(0,n_L)$ $(k_s,0)(k_m,n_m)$ $(k_s,0)(k_L,-n_L)$ $(k_s,-n_m)(k_m,n_m)$	V1	$(0,0)(k_s,-n_L)$ $(0,0)(k_m,-n_L)$ $(k_s,0)(k_m,n_L)$ $(k_s,0)(k_m,n_m)$ $(k_s,-n_m)(k_m,n_m)$
$(k_s,0)(k_s,n_L)$	V2	$(k_s,0)(k_m,n_L)$ $(k_s,\pm n_L)(k_m,\mp n_L)$ $(k_m,-n_h)(k_L,-n_h)$

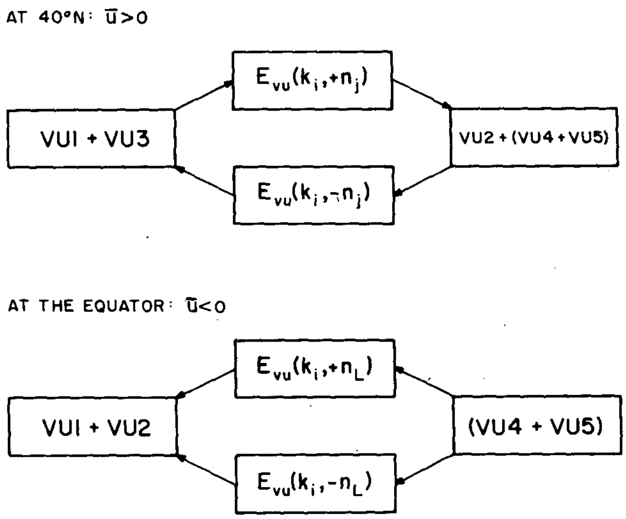

FIG. 10. Schematic diagram for the maintenance of the spectral meridional flux of westerly momentum in moving waves at 500 mb, winter 1973.

flux of westerly momentum in wavenumber-frequency domains is directed toward the north at 20°N and 40°N, but toward the south at 20°S. At the equator the spectral flux of westerly momentum is generally small, and varies its direction in different wavenumber-frequency domains.

2) Except for the eastward slowly moving waves of medium wavelengths at 40°N, the resultant of the nonlinear interactions corresponding to the longitudinal convergence of the meridional flux of westerly momentum ($VU1$) in wavenumber-frequency domains provides a northward flux of westerly momentum in eastward moving waves but a southward flux of momentum in westward moving waves at 20°N and 40°N. The reverse is true at 20°S. At the equator, the nonlinear contribution of $VU1$ is generally small, and varies its sign in different wavenumber-frequency domains.

3) The resultant of the nonlinear interactions corresponding to the latitudinal convergence of the meridional flux of westerly momentum ($VU2$) is generally small and is of opposite sign to that corresponding to the longitudinal convergence of the meridional flux of westerly momentum ($VU1$).

4) The combined contribution of the pressure, Coriolis and Reynolds stress forces (including computational errors), i.e., ($VU4+VU5$), is generally of the opposite sign to the nonlinear interaction contributions corresponding to the longitudinal convergence of the meridional flux of westerly momentum ($VU1$).

5) The effect of the earth's sphericity ($VU3$) is generally small.

Fig. 10 schematically shows the maintenance of the spectral meridional flux of zonal momentum as the resultant of the nonlinear interactions, and the pressure, Coriolis and Reynolds stress forces. At 40°N in the westerlies, the nonlinear interactions [($VU1+VU3$) corresponding to the longitudinal convergence of the meridional flux of westerly momentum and the effect of sphericity] supply (extract) spectral meridional flux of zonal momentum to (from) eastward (westward) moving waves, whereas the pressure, Coriolis, and Reynolds stress forces (including computational errors), i.e., ($VU4+VU5$), and the nonlinear interactions [($VU2$) corresponding to the meridional convergence of the momentum flux] extract (supply) spectral momentum flux from (to) eastward (westward) moving waves. At the equator in the easterlies, however, the pressure and Reynolds stress forces (including computational errors), i.e., ($VU4+VU5$), supply spectral momentum to both the eastward and westward moving waves, whereas the nonlinear interactions [($VU1+VU2$) corresponding to the longitudinal and meridional convergence of momentum flux] extract spectral momentum flux from both the eastward and westward moving waves.

TABLE 7. Linear and nonlinear contributions to the meridional flux of westerly momentum per unit mass in various wavenumber-frequency domains at 20°S, the equator, 29°N and 40°N at 500 mb.

		EVU	=	VU1	+ VU2	+ VU3	+ (VU4+VU5)
$(k_s, +n_L)$	40°N	7.65	=	29.12	-27.95	+ 2.34	+ 4.14
	20°N	2.59	=	7.62	- 0.43	+ 0.46	- 5.06
	0	0.11	=	-0.25	- 0.01	+ 0.00	+ 0.37
	20°S	-0.14	=	- 0.37	+ 0.42	+ 0.16	- 0.36
$(k_s, -n_L)$	40°N	3.67	=	- 6.03	+17.51	- 9.02	+ 1.21
	20°N	1.40	=	- 8.28	- 2.01	+ 0.08	+11.61
	0	0.17	=	- 0.29	- 0.35	+ 0.00	+ 0.80
	20°S	-0.37	=	0.08	- 0.62	+ 0.09	+ 0.08
$(k_s, +n_m)$	40°N	3.12	=	5.74	+ 0.68	+ 0.27	- 3.57
	20°N	0.32	=	0.22	+ 0.07	+ 0.00	+ 0.03
	0	-0.01	=	0.01	+ 0.00	+ 0.00	- 0.02
	20°S	-0.01	=	- 0.02	+ 0.01	+ 0.00	- 0.01
$(k_m, +n_L)$	40°N	-5.13	=	-20.60	+ 2.10	- 0.09	+13.46
	20°N	1.04	=	6.13	- 0.55	- 0.18	- 4.37
	0	0.04	=	- 0.25	+ 0.01	+ 0.00	+ 0.28
	20°S	-1.06	=	- 2.48	+ 0.17	- 0.01	+ 1.26
$(k_m, -n_L)$	40°N	0.39	=	- 8.34	+ 1.40	+ 0.57	+ 6.76
	20°N	0.06	=	- 2.08	- 0.27	+ 0.02	+ 2.39
	0	-0.09	=	- 0.05	- 0.13	+ 0.00	+ 0.09
	20°S	-0.43	=	1.15	- 0.05	+ 0.07	- 1.59
$(k_m, +n_m)$	40°N	5.18	=	12.53	- 2.84	+ 0.01	- 4.52
	20°N	0.94	=	0.93	+ 0.09	+ 0.00	- 0.09
	0	0.02	=	- 0.00	+ 0.00	+ 0.00	+ 0.02
	20°S	-0.15	=	- 0.16	- 0.03	- 0.00	+ 0.04

In Tables 8–10, the primary and secondary nonlinear interaction contributions to the longitudinal and latitudinal convergence of the meridional flux of westerly momentum at the equator, 20°N and 40°N are summarized. In these tables, the primary (underlined) and secondary interactions are, respectively, classified according to interaction values being greater than 0.5 and between 0.15 and 0.5 $m^2 s^{-2}$ for interactions at the equator, greater than 2.0 and between 0.5 and 2.0 $m^2 s^{-2}$ at 20°N, and greater than 10.0 and between 2.0 and 10.0 $m^2 s^{-2}$ at 40°N.

It may be noted in Tables 8–10 that nonlinear contributions to the longitudinal and latitudinal convergence of the meridional flux of westerly momentum involve primarily the low-frequency waves of long and medium wavelengths interacting with the zonal mean flow and with the stationary long waves. At 40°N, however, interactions between eastward and westward moving long waves of low frequencies also contribute substantially to the meridional flux of westerly momentum.

10. Summary and conclusions

An analysis of the mechanism for the large-scale wave motion in the atmosphere in the wavenumber-frequency domain indicates that the large-scale atmospheric waves of same wavelengths can have many phase velocities, and that the nonlinear interactions transfer kinetic energy to waves of various wavelengths and phase velocities.

Specifically, the nonlinear interactions generally supply kinetic energy to waves moving in the direction of the mean zonal flow, but extract kinetic energy from waves moving in the opposite direction of the mean zonal flow. In the middle latitudes, the pressure force

TABLE 8. Summary of positive and negative nonlinear contributions to *VU*1 and *VU*2 in various wavenumber-frequency domains at the equator at 500 mb.

Positive Contributions		Negative Contributions
$(0,0)(k_s,-n_L)$		$(k_s,0)(k_s,n_L)$
$(0,0)(k_m,-n_L)$		$(k_s,0)(k_m,-n_L)$
$(k_s,0)(k_s,-n_L)$		$(0,0)(k_m,n_L)$
$(k_s,0)(k_m,n_L)$	→ VU1 →	$(0,0)(k_L,n_L)$
$(k_s,0)(0,n_L)$		$(0,n_L)(k_m,-n_L)$
$(k_s,n_L)(k_s,-n_L)$		$(k_s,0)(k_m,n_L)$
$(k_s,n_L)(k_m,0)$		$(k_s,0)(k_L,-n_L)$
$(k_m,0)(k_m,\pm n_L)$		$(k_L,n_L)(k_m,n_L)$
$(k_m,-n_L)(k_m,-n_L)$		$(k_m,0)(k_s,n_L)$
$(k_s,-n_m)(k_m,-n_m)$		

Positive Contributions		Negative Contributions
$(k_s,0)(k_s,-n_L)$	→ VU2 →	$(0,n_L)(k_s,0)$
$(k_s,0)(k_m,-n_L)$		
$(k_s,0)(0,-n_L)$		
$(k_s,-n_L)(k_s,\pm n_L)$		
$(k_m,0)(k_m,n_L)$		
$(k_m,-n_L)(k_m,-n_L)$		

TABLE 9. As in Table 8 except at 20°N.

Positive Contributions		Negative Contributions
$(k_s,0)(k_s,n_L)$		$(k_s,0)(k_s,-n_L)$
$(0,0)(k_s,-n_L)$		$(0,0)(k_s,n_L)$
$(0,0)(k_L,-n_L)$	→ VU1 →	$(0,0)(k_m,n_L)$
$(k_s,0)(k_s,-n_L)$		$(k_s,0)(k_L,\pm n_L)$
$(k_s,0)(k_m,-n_L)$		$(0,\pm n_L)(k_s,\mp n_L)$
$(k_s,0)(0,-n_L)$		$(k_s,+n_L)(k_s,-n_L)$
$(k_s,-n_L)(k_s,-n_L)$		
$(k_s,-n_L)(k_m,-n_L)$		
$(k_m,-n_L)(k_m,-n_L)$		
$(k_m,-n_L)(k_L,-n_L)$		
$(k_L,-n_L)(k_L,-n_L)$		

Positive Contributions		Negative Contributions
$(k_s,0)(k_s,-n_L)$	→ VU2 →	$(k_s,0)(0,-n_L)$
$(k_s,0)(k_m,-n_L)$		
$(k_s,+n_L)(k_s,-n_L)$		

TABLE 10. As in Table 8 except at 40°N.

Positive Contributions		Negative Contributions
$(0,0)(k_s,n_L)$		$(0,0)(k_m,\pm n_L)$
$(k_s,+n_L)(k_s,-n_L)$		$(k_s,0)(k_s,n_L)$
$(0,0)(k_s,n_m)$		$(k_s,0)(k_m,n_L)$
$(0,0)(k_m,n_m)$		$(0,0)(k_s,-n_L)$
$(k_s,0)(0,-n_L)$		$(0,n_L)(k_s,-n_L)$
$(k_s,0)(k_m,n_L)$	→ VU1 →	$(k_s,0)(k_s,-n_L)$
$(0,-n_L)(k_s,n_L)$		$(k_s,0)(k_m,-n_L)$
$(0,-n_L)(k_m,n_L)$		$(k_s,\pm n_L)(k_m,\mp n_L)$
$(k_s,n_L)(k_s,\pm n_L)$		$(k_m,+n_L)(k_m,-n_L)$
$(k_s,-n_L)(k_m,n_L)$		$(k_L,+n_m)(k_L,-n_m)$
$(k_s,-n_L)(k_m,n_m)$		
$(k_m,n_h)(k_m,-n_h)$		

Positive Contributions		Negative Contributions
$(k_s,0)(k_s,-n_L)$		$(k_s,0)(k_s,n_L)$
$(k_s,0)(0,n_L)$		$(k_s,-n_L)(k_m,n_L)$
$(k_s,0)(k_m,-n_L)$		$(k_s,0)(k_m,n_L)$
$(k_s,n_L)(k_s,n_L)$		$(0,-n_L)(k_L,n_L)$
$(k_s,n_L)(k_m,-n_L)$		$(k_s,n_L)(k_m,-n_L)$
$(k_s,n_m)(k_s,-n_m)$		$(k_m,-n_L)(k_L,n_L)$
$(k_m,n_L)(k_m,-n_m)$	→ VU2 →	$(k_L,n_m)(k_L,-n_m)$
$(k_m,-n_m)(k_L,n_m)$		
$(k_m,-n_h)(k_m,n_h)$		
$(k_m,-n_h)(k_L,n_h)$		
$(k_L,-n_h)(k_L,n_h)$		

supplies kinetic energy to waves moving in the opposite direction of the mean zonal flow, but extracts kinetic energy from waves moving in the direction of the mean zonal flow. Near the equator, however, the pressure supplies kinetic energy to both eastward and westward moving waves.

The primary contribution of the nonlinear interactions to the energy transfer in wavenumber-frequency domain is essentially through the interactions of the slowly moving waves, the stationary long waves and the zonal mean flow. The interactions between the stationary long waves and waves moving in the same (opposite) direction of the mean zonal flow generally extract (supply) kinetic energy from (to) the moving waves, whereas the interactions between the mean zonal flow and waves moving in the same (opposite) direction of the mean zonal flow generally supply (extract) kinetic energy to (from) the moving waves.

It is seen from the analysis of the linear and nonlinear interactions that the maintenance of the large-scale wave motion in the atmosphere is more complex than that of the microscale waves of which the kinetic energy is primarily maintained through the cascade of kinetic energy from the energy containing eddies to eddies in the dissipation range.

Acknowledgment. This research was partly supported by the Global Atmospheric Research Program of the National Science Foundation under Grant GA 40387.

REFERENCES

Bedient, H. A., W. G. Collins and G. Dent, 1967: An operational tropical analysis system. *Mon. Wea. Rev.*, **95**, 942–949.

Charney, J. G., 1971: Geostrophic turbulence. *J. Atmos. Sci.*, **28**, 1087–1095.

Gruber, A., 1975: The wavenumber-frequency spectra of the 200 mb wind field in the tropics. *J. Atmos. Sci.*, **32**, 1615–1625.

Hayashi, Y., 1971: A generalized method of resolving disturbances into progressive and retrogressive waves by space Fourier and time cross-spectral analysis. *J. Meteor. Soc. Japan*, **49**, 125–128.

Kao, S.-K., 1968: Large-scale atmospheric motion and transports in frequency wave-number space. *J. Atmos. Sci.*, **25**, 32–38.

——, 1970: The wavenumber-frequency spectra of temperature in the free atmosphere. *J. Atmos. Sci.*, **27**, 1000–1007.

——, and Wendell, L. L., 1970: The kinetic energy of the large-scale atmospheric motion in wavenumber-frequency space. I. Northern Hemisphere. *J. Atmos. Sci.*, **27**, 359–375.

——, C.-Y. Tsay and L. L. Wendell, 1970: The meridional transport of angular momentum in wavenumber-frequency space. *J. Atmos. Sci.*, **27**, 614–626.

Koopmans, L. H., 1974: *The Spectral Analysis of Time Series*. Academic Press, 366 pp.

Kraichnan, R. H., 1967: Inertial range in two-dimensional turbulence. *Phys. Fluids*, **10**, 1417–1423.

Leith, C. E., 1968: Diffusion approximation for two-dimensional turbulence. *Phys. Fluids*, **11**, 671–672.

——, 1971: Atmospheric predictability and two-dimensional turbulence. *J. Atmos. Sci.*, **28**, 145–161.

Lily, D. K., 1969: Numerical simulation of two-dimensional turbulence. *Phys. Fluids*, **12** (Suppl. II), 240–249.

Lorenz, E. N., 1967: The nature and theory of the general circulation of the atmosphere. WMO No. 218, TP. 115, 161 pp.

Pratt, R. W., 1976: The interpretation of space-time spectral quantities. *J. Atmos. Sci.*, **33**, 1060–1066.

Steinberg, H. L., A. Wiin-Nielsen and C. -H. Yang, 1971: On nonlinear cascades in large-scale atmospheric flow. *J. Geophys. Res.*, **76**, 8629–8640.

Tsay, C. Y., 1974a: A note on the methods of analyzing traveling waves. *Tellus*, **26**, 412–415.

——, 1974b: Analysis of large-scale wave disturbances in the tropics simulated by an NCAR global circulation model. *J. Atmos. Sci.*, **31**, 330–339.

Tukey, J. W., 1967: Spectrum calculations in the new world of the fast Fourier transform. *Advanced Seminar on Spectral Analysis of Time Series*, B. Harris, Ed., Wiley, 25–46.

Wendell, L. L., 1969: A study of the large-scale atmospheric turbulent kinetic energy in wavenumber-frequency space. *Tellus*, **21**, 760–788.